Short-term evolution of antibiotic responses in highly dynamic environments favors loss of regulation.

John Crow, Hao Geng, Daniel Schultz*

Department of Microbiology & Immunology, Dartmouth – Geisel School of Medicine, Hanover, NH, USA.

* Correspondence:

Daniel.Schultz@dartmouth.edu

Abstract

Microbes inhabit natural environments that are remarkably dynamic, with sudden environmental shifts that require immediate action by the cell. To cope with changing environments, microbes are equipped with regulated response mechanisms that are only activated when needed. However, when exposed to extreme environments such as clinical antibiotic treatments, complete loss of regulation is frequently observed. Although recent studies suggest that the initial evolution of microbes in new environments tends to favor mutations in regulatory pathways, it is not clear how this evolution is affected by how quickly conditions change (i.e. dynamics), or which mechanisms are commonly used to implement new regulation. Here, we perform experimental evolution on continuous cultures of *E. coli* carrying the tetracycline resistance *tet* operon to identify specific types of mutations that adapt drug responses to different dynamical regimens of drug administration. When cultures are evolved under gradually increasing tetracycline concentrations, we observe no mutations in the *tet* operon, but a predominance of fine-tuning mutations increasing the affinity of alternative efflux pump AcrB to tetracycline. When cultures are instead periodically exposed to large drug doses, all populations developed transposon insertions in repressor TetR, resulting in loss of regulation of efflux pump TetA. We use a mathematical model of the dynamics of antibiotic responses to show that sudden exposure to large drug concentrations can overwhelm regulated responses, which cannot induce resistance fast enough, resulting in fitness advantage for constitutive expression of resistance. These results help explain the loss of regulation of antibiotic resistance by opportunistic pathogens evolving in clinical environments. Our experiment supports the notion that initial evolution in new ecological niches proceeds largely through regulatory mutations and suggests that transposon insertions are a main mechanism driving this process.

Introduction

When microbes colonize new ecological niches, they must adapt their responses to the specific demands of the new environment[1–4]. Microbes are typically equipped with inducible mechanisms that sense changes in their surroundings and initiate the appropriate cellular programs[5–7]. In some cases, the initiation of responses is not time sensitive and mostly tunes the expression of relevant genes to optimal levels, such as when cells respond to shifts in nutrient conditions[8,9]. But in situations where cells are exposed to antibiotics or other harmful compounds, cell survival depends on the ability to deploy its defenses quickly, while gene expression is still possible[10,11]. Therefore, even if a cell carries the appropriate mechanisms to deal with a hostile environment, sudden and frequent changes in conditions still challenge cells that are too slow to respond.

Dynamic environments pose fundamentally different selective pressures in the evolution of antibiotic responses[10,12–14]. Antibiotic resistance mechanisms originate in the soil, which typically harbors low drug concentrations[15]. In such environments, antibiotics are thought to be present within a selection window that inhibits the growth of sensitive strains while enriching resistant subpopulations, which encourages the emergence of multiple beneficial mutations[16,17]. On the other hand, antibiotics are used in the clinic with the intent of wiping out entire microbial populations[18]. Sudden exposures to high drug doses then select for the few surviving mutants, however unfit, while eliminating any potential competitors[19–23]. Such extreme environments can pose strict bottlenecks resulting in the selective sweeps of single mutations that are not optimal but are more likely to occur[24,25]. While much attention has been devoted to the evolution of antibiotic resistance, this evolution is mostly studied in sensitive strains under steady drug concentrations[26]. To anticipate the evolution of antibiotic resistance in the clinic, it is necessary to understand the general mechanisms guiding evolution in dynamic environments, where antibiotic concentrations are high and change quickly.

Recent studies suggest that the short-term evolution of microbes in new environments relies heavily in mutations affecting regulatory pathways[27–31]. To study the dynamics of induction of antibiotic responses, we focus on tetracycline resistance in *E. coli*. The ancestral WT strain we used in our evolution experiments possesses two inducible efflux mechanisms capable of transporting tetracycline out of the cell - the *tet* and *acr* operons (Fig. 1A). While the *acr* operon transports a wide variety of toxic compounds and is part of the *E. coli* core genome, the *tet* operon is a tetracycline specific optional mobile element, providing the bulk of resistance in strains where it is present[32,33]. Both mechanisms are regulated by repressors of the same family - TetR and AcrR, respectively – which are known to recognize the same ligands as the efflux pumps they regulate[34–37]. Upon binding the drug, the affinity of the repressors for their DNA binding sites is greatly diminished, releasing expression of their respective efflux pumps, TetA and AcrAB, which then actively transport tetracycline out of the cytoplasm[37–39]. Since the *acr* operon is not optimized for tetracycline, several mutations in *acrB* have been reported to increase tetracycline resistance[32,40–42]. Active transport the *tet* operon involves an ion exchange that has been shown to disrupt the membrane potential, thereby posing a trade-off between resistance to tetracycline and the adverse effects of TetA expression[10,38,39]. Therefore, tetracycline resistance depends on the interaction between two inducible

mechanisms, with different costs/benefits and drug specificities, and resistance can be increased by acquiring mutations in either one.

Here, we use a system of automated continuous cultures to experimentally evolve tetracycline resistant *E. coli* populations under different dynamic regimens of drug administration. Continuous cultures offer the advantage of precise control of drug concentration while keeping population growth for many days[43]. We compare evolution under a steady drug environment, where the drug concentration changes gradually, with a fast-changing environment where the population is periodically subjected to sudden exposures to high drug concentrations. While steady environments are expected to favor mutations that maximize growth under high drug concentrations, fast-changing environments should pose a strict bottleneck that selects mutants that can quickly recover growth following drug exposures. We then analyze the evolved populations in each of these conditions to determine how the dynamics of the environment dictates the evolution of resistance, particularly with regards to the regulation of drug responses.

Results

We have developed a device for microbial evolution in controlled dynamic environments, based on the morbidostat design, which propagates continuously growing cultures while automatically adjusting media input and antibiotic concentration to impose specific regimens of drug administration to an evolving microbial population[44]. The device allows the maintenance of cultures at a set density by measuring turbidity (optical density) in real time and externally adjusting media and drug delivery via a control algorithm. Our device does not elevate drug concentration in a predefined way but, rather, automatically adjusts drug concentration to impose regimens with desired dynamic characteristics. We used our setup to impose both the “Steady” and “Dynamic” environments to the evolved populations, implemented by different control algorithms.

Steady environment favors mutations adapting AcrB to tetracycline.

Most studies performing experimental evolution of antibiotic resistance have focused on the acquisition of resistance by sensitive strains, while less attention has been given to the evolution of strains carrying dedicated mechanisms of resistance[45]. Previous studies with sensitive *E. coli*, which carries the unoptimized *acr* but not the *tet* operon, have shown that increasing concentrations of tetracycline in chemostats can evolve 10-fold higher resistance over the course of two weeks[43]. Due to the high fitness costs of mutations in the ribosome, the drug target, most adaptive mutations in these studies were found in genes coding for membrane proteins, including the *acr* operon, or factors affecting transcription and translation. In comparison, *tet*+ strains achieve much higher resistance, with an MIC 100-fold larger than sensitive strains[10]. Since the *tet* operon confers the bulk of tetracycline resistance, it was unclear if the evolution of *tet*+ strains would proceed in the same fashion. If the *tet* operon could be further optimized for higher doses of tetracycline, mutations the *tet* genomic locus were likely to have large effects on resistance. On the other hand, narrow-spectrum mechanisms such as the *tet* operon can be expected to already be highly optimized for their preferred antibiotic substrates. In this case, adaptive mutations were expected elsewhere, either providing resistance through

other means or compensating for fitness costs associated to high expression of the *tet* operon.

To determine the evolution of *tet*-resistant strains to high doses of tetracycline, we evolved 3 resistant populations (Std-1, Std-2 and Std-3) under gradually increasing drug levels following the morbidostat design (Fig 1B). In this "Steady" regimen, we used 15 ml of cell cultures at a fixed dilution rate of 0.35 h^{-1}, added every 5 minutes, which corresponds to a growth rate of 0.5 doublings per hour and an OD (optical density) of 0.15 for the ancestral strain in the absence of drug. Tetracycline was automatically added to the cultures in increments of 4.4 µg/ml in every cycle where the population showed net growth over the previous 30 minutes. This regimen initially resulted in cell densities between 0.2 and 0.3, while keeping a constant selective pressure resulting from drug inhibition of growth. Under these conditions, the drug is always present, with levels gradually increasing as the population evolves resistance. Since there is no need to repress expression of TetA, we expected that adaptation would proceed by fine tuning TetA levels to high drug concentrations, with little necessity for TetR repression.

Within a few days, all populations quickly adjusted to growth at higher drug doses. After 3 days, all 3 populations were growing stably with OD around 0.3 and drug concentrations above 500 µg/ml (Fig 1C, SI). To analyze the progression of drug resistance in each population throughout the experiment, we inoculated a sample from each day in a gradient of tetracycline, measuring the drug concentration that reduces growth in half in comparison with the absence of drug (IC_{50}). By the third day, all 3 populations had developed high levels of resistance (Fig 1DE). Samples were collected daily during the experiment. On completion, gDNA from each final culture was extracted and sent for whole genome sequencing, together with the ancestral WT population (MG1655 *tet*+), to identify adaptive mutations by aligning WGS reads to a reference genome. We also sequenced a culture evolved in a turbidostat in the absence of drug to identify possible mutations that are adaptive to growth under our experimental conditions, but not related to drug resistance. We did not find any significant such mutations.

All three steady cultures evolved genetically diverse populations (Table 1), with significantly increased resistance in comparison to the wild type. We did not find any mutations in the *tet* operon locus, suggesting that TetA is already highly optimized for growth under high levels of tetracycline. Instead, we observed a predominance of mutations enhancing other mechanisms of resistance. In particular, we found many mutations in the *acr* operon. All three populations acquired mutations disrupting the regulation of AcrB, either by disrupting repressor AcrR or the *acrRAB* promoter region. Additionally, two populations acquired mutations in the drug binding pocket of the AcrB protein itself[40,46,47], which presumably increase the affinity of AcrB to tetracycline (Fig 1F). Therefore, the alternative mechanism of tetracycline efflux provided by AcrB complements resistance provided by TetA, and becomes the focus of evolution since it was not previously optimized for tetracycline in the WT.

We also observed other mutations that potentially reduce membrane permeability to tetracycline, such as in porin regulator OmpR and in PlsB and YhdP, involved in phospholipid synthesis and transport[48,49]. In all evolved populations, we also detected a low abundance of several mutations related to transposable elements, which might

provide an efficient mechanism to generate additional mutants. Interestingly, population Std-3 showed two mutations upstream of 16S subunit ribosomal RNA *rrsG*, the target of tetracycline, which possibly upregulate expression levels in response to the drug. In populations Std-1 and Std-3, we found fixation of a large deletion of chemotaxis and motility genes, which was already detected in low abundance in the ancestral WT population. Since overexpression of efflux pump TetA is known to have deleterious effects from depleting the membrane potential, we speculate that the deletion or inactivation of several motor proteins involved in motility might provide a mechanism to alleviate the toxic effects of constant TetA expression.

To study the emergence of competing lineages in the evolving populations, we selected the genes with the most abundant mutations in the evolved populations for further analysis: *plsB* (Std-1), *acrB* (Std-2 and Std-3) and *ompR* (Std-2 and Std-3). We picked 5 isolates for each population for each day of the experiment and determined the presence of each mutation by Sanger sequencing. We then used these data to determine the order and co-occurrence of mutations within the same lineage and infer a phylogenetic tree of the competing lineages for the duration of the experiment (Fig 1G). Surprisingly, we found an abundance of alternative mutations in the *acr* operon that were not detected in the final populations. In all populations, we found that mutations affecting AcrB regulation preceded mutations in AcrB itself. This result suggests that tetracycline is not an effective inducer of the *acr* operon, and disruption of AcrR repression is necessary to activate AcrAB expression and potentialize further mutations in *acrB*. In both populations Std-2 and Std-3, we found an initial competition between several *acr* regulatory mutations, followed by competition between several *acrB* mutations. In population Std-1, we only detected an *IS2* transposon insertion within the *acrRAB* promoter region, and no other further mutations anywhere in the *acr* operon. The *IS2* insertion sequence is known to introduce a strong promoter that can result in upregulation of adjacent genes[50,51], so we speculate that particularly high expression of AcrB in Std-1 resulted in a fit mutant that inhibited the emergence of competing lineages. But in general, we conclude that evolution in steady drug regimens first acts on regulatory pathways to ensure upregulation of resistance mechanisms, then acts on resistance proteins themselves, optimizing affinity to the specific drug in question.

Dynamic environment favors loss of *tet* regulation.

The majority of studies on the experimental evolution of antibiotic resistance have focused on evolution under steadily increasing antibiotic concentrations, which does not account for the dynamic nature of many natural habitats such as clinical settings[45]. In these environments, while drug exposures can be relatively rare, they happen suddenly. Therefore, apart from reducing the burden of constant expression, the regulation of resistance mechanisms also needs to deliver fast responses upon sudden shifts in drug concentration. At first thought, evolution in such highly dynamic environments should lead to faster induction of resistance, so cells can quickly adapt to the presence of the drug while still avoiding unnecessary expression when the drug is removed. However, faster responses might depend on rare mutations that cannot be quickly achieved under the strict evolutionary bottlenecks imposed by sudden exposures to high drug doses. Therefore, it was unclear if faster regulation of the *tet* operon would be a likely outcome of evolution in such environments.

To determine the role of dynamics in the evolution of drug responses, we evolved three resistant populations under fast-changing drug environments (Dyn-1, Dyn-2 and Dyn-3), implemented by controlling drug delivery in a turbidostat (Fig 2A). In this setup, we kept 15 ml of cell culture at a fixed target OD of 0.15 by the controlled dilution of the culture with drug-free media. Every 24 hours cultures were exposed to a single large dose of tetracycline by the addition of 15 ml of medium with drug, which also caused the population to be diluted by half. We then waited for the culture to recover to the target OD without dilution. Following recovery, controlled addition of fresh medium resumed and the drug concentration gradually decreased to zero (Fig 2B). We started with an exposure to 150 μg/ml of tetracycline in the first day, which was shown to cause significant delays in recovery from drug exposure in the ancestral WT population. The drug concentrations for subsequent exposures were calculated based on the recovery time from the previous exposure, with concentrations increasing if the recovery time was shorter than 5 hours. If a culture did not fully recover within 24 hours, no drug was added to that culture in that cycle. The dynamic adjustment of the shock dose maintains evolutionary pressure for faster response times, while the fast-growth condition after drug is diluted following recovery provides a fitness advantage for cells that grow efficiently in the absence of drug. A regimen of daily administration of the drug was chosen to provide enough time for growth in drug-free conditions and to reflect typical timescales of antibiotic treatments.

All three populations quickly recovered from the first exposure, and were followed by significant increases in drug dose for the exposures in the following days. Recovery times were higher within the first few days, but eventually stabilized at around 45 to 60 minutes by the end of the experiment (Fig 2C, SI). In general, populations recovered quickly and showed fast growth following drug exposures, which resulted in fast dilution rates and ensured that the drug was removed from the culture within 10 hours. However, two populations, Dyn-1 and Dyn-3, recovered quickly from the first exposure, resulting in a large increase in the drug dose for the second exposure. This led to slow growth and a long recovery time, so the third exposure was skipped. Eventually, these populations also evolved fast growth and quick recovery times. Next, we measured the progression of drug resistance in each population throughout the experiment. Overall, all 3 Dynamic populations were slower to develop resistance in comparison to the Steady populations, as measured by the IC_{50}, with populations Dyn-1 and Dyn-3 being slower than Dyn-2 (Fig 2DE). These results support the notion that the strict evolutionary bottlenecks imposed by the Dynamic environment might select mutants that are less fit in comparison to the Steady environment. Again, samples were collected on a daily basis, and were sent for whole genome sequencing at the end of the experiment. As with the Steady drug regimen, the Dynamic regimen produced genetically diverse populations with significantly increased resistance (Table 2).

Unexpectedly, instead of evolving fast on/off switching of the drug response, all Dynamic populations independently acquired transposon insertions in the *tetR* gene, abolishing regulation of efflux pump TetA. Each population acquired a transposable element *IS5* insertion in a different genomic site inside the *tetR* gene. We verified the presence of these in each population throughout the experiment by PCR and found that *IS5* insertions in *tetR* rapidly arose and reached fixation in populations Dyn-1 and Dyn-2 (Fig 2F, SI). In population Dyn-3, *tetR* insertions only rose in frequency in the last few days but did not

reach fixation. Such insertions result in loss of TetR function, and therefore TetA expression is permanently de-repressed. Still, in the presence of the drug, fully induced TetA levels are similar between WT cells and *tetR* mutants. These results suggest that constitutive expression of TetA improves resistance by bypassing the process of induction of the drug response, and therefore we hypothesize that preemptive expression of resistance might shorten population-level recovery despite the known fitness costs of TetA overexpression.

In all populations, we also observed a high abundance of *acr* operon regulatory mutations. Notably, we did not find any mutations in the *acrB* gene. Populations Dyn-1 and Dyn-2 both showed *IS1* transposon insertions in *acrR*, and population Dyn-3 showed both mutations in the *acrRAB* promoter and in *acrR* itself. Therefore, optimization of the alternative resistance mechanism provided by AcrB also increases fitness in the Dynamic environment. Again, we observed other prevalent mutations that potentially reduce membrane permeability to tetracycline or compensate for its effects. Population Dyn-2 showed a mutation in RNA polymerase subunit *rpoB* and in the *kgtP* transporter. Population Dyn-3 showed a mutation in porin regulator *ompR.* We also found several mutations related to transposable elements. In populations Dyn-1 and Dyn-2, we also found the fixation of the large deletion of chemotaxis and motility genes. If indeed this deletion of multiple protein motors help compensate for TetA overexpression, its absence in population Dyn-3 might help explain why the *tetR* insertion was slower to rise in abundance.

Again, we picked 5 isolates for each population for each day of the experiment and determined the presence of the most abundant mutations in the evolved populations: *acrR* (Dyn-1, Dyn-2 and Dyn-3), *rpoB* (Dyn-2) and *ompR* (Dyn-3). We then determined co-occurrence of mutations within the same lineages and inferred their phylogenetic tree (Fig 2G). In all populations, *tetR* insertions preceded any other mutations (including Dyn-3) and were inevitably followed by mutations upregulating the *acr* operon within the same lineage. In population Dyn-1 no other abundant mutations were found, and in population Dyn-2 a *rpoB* mutation arose only at the end of the experiment. In population Dyn-3, although a *tetR* insertion was detected early, by day 4 it was competing with another lineage carrying mutations in *ompR* and in the *acRAB* promoter. The lineage with the *tetR* insertion then developed two competing *acr* regulatory mutations before rising to ~30% abundance in the last 4 days of the experiment. Therefore, although lineages with *tetR* insertions were either fixated or rising in frequency by the end of the experiment, mutations outside of the *tet* operon can also significantly increase fitness in dynamic environments and compete against the emergence of *tetR* mutants.

We note that the dynamic environments could promote the coexistence of multiple mutants that are specialized to different drug levels. In the dynamic environment, when a population recovers growth following an exposure, however slowly, drug begins to be removed from the medium. The resulting lower drug levels can then allow the recovery of faster-growing lineages that would not have grown under the peak drug concentration. Therefore, highly resistant low-growth mutants can aid the evolution of more fit mutants in this context by lowering drug levels following exposure. For instance, this could have happened in the second exposure of populations Dyn-1 and Dyn-3, which resulted in low growth. The slow-growing mutants would then have been present in these populations

around day 3 - where we did not find any of the mutations present in the final populations - but would have likely been replaced by faster growing mutants within the following few exposures. To confirm this hypothesis, we plan on further analyzing the Dyn-1 and Dyn-3 isolates from day 3 in the future. Next, we moved to study the dynamics of the response in the relevant mutants, to understand the population dynamics of the evolving populations.

Mutations optimizing *acrB* provide highest resistance and shortest recoveries.

To measure the performance of antibiotic resistance in the evolved populations during abrupt changes in drug concentration, we performed a liquid-culture assay to assess the dynamics of population-level growth during drug responses (Fig. 3A). When growing liquid cultures are suddenly exposed to high drug concentrations, growth defects appear in the transient following exposure, as a fraction of the cells is arrested[10]. At the population level, an initial pause in growth is observed, followed by recovery when a growing population rises above the background of arrested cells. The speed of recovery following exposure to tetracycline, accounting for both cell death and slow growth, can be measured as the delay in the time it takes to achieve one doubling due to the presence of drug. Both the speed of recovery from the transient and the steady-state growth rate decline as a function of drug concentration. We then quantify resistance using two components: “steady-state resistance”, which measures the capacity for bulk growth in the presence of drug (similar to IC_{50}), and “dynamical resistance”, which measures the speed of recovery upon exposure (methods, SI).

While all populations evolved similar levels of steady-state resistance, we found significant differences in dynamical resistance. Surprisingly, the populations evolved in the dynamical regimen showed generally lower dynamical resistance than the populations evolved in the steady regimen (Fig. 3A). This result suggests that the mutations acquired under steady drug conditions, adapting the cell to grow under constant drug pressure, can also shorten population recovery following drug exposures. We also note that the evolved populations grow faster in the presence of moderate concentrations of tetracycline than in its absence (SI). Since the evolved populations are diverse and can harbor the coexistence of mutants with different resistance profiles, we also assessed resistance in a collection of isolates from the final evolved populations. We found that while all isolates from populations evolved in the dynamic regimen displayed significant dynamical resistance, the highest dynamical resistance was measured in isolates from population Std-2 combining mutations in *acrB* and *ompR*. Therefore, mutations that increase the affinity of *acrB* to tetracycline, improving the efficiency of tetracycline efflux, are likely to result in both faster recovery from drug exposure and steady-state growth at higher drug concentrations. Meanwhile, regulatory mutations that shorten recovery from exposure, such as *tetR* transposon insertions, do not necessary result in growth at higher drug levels.

Sudden exposures to high drug doses overwhelm regulated responses

To understand the fitness advantage provided by loss of *tetR* repression, we picked isolates from the same early Dynamic populations where *tetR* insertions first emerged. We then compared how isolates with and without *tetR* insertions respond to sudden

exposures to high doses of tetracycline (Fig. 4A, SI). When liquid cultures of these isolates were exposed to a step increase in tetracycline, populations with *tetR* insertions recovered growth much earlier, despite little change in the steady-state growth rate once growth was recovered. Therefore, abolishing TetR repression of TetA promotes survival of the initial exposure and recovery of growth among single cells, but steady-state growth under full TetA induction is similar between WT and *tetR* mutants.

Once *tetR* mutations are acquired, activation of *acrB* resistance through regulatory mutations provide further gains both in recovery speed and in steady-state growth under the drug. We measured dynamical and steady-state resistance in WT isolates, *tetR* mutants and also in *tetR* mutants that acquired further a further mutation disabling AcrR (Fig. 4B). *tetR* insertions increased dynamical resistance substantially, as expected, but also provided a slight increase in steady-state resistance. Since we did not observe differences in steady-state growth rates between WT and *tetR* mutants for any drug concentration where they are both viable (SI), this short window of drug concentrations where only the *tetR* mutants grow likely results from WT cells no longer being able to fully induce TetA expression in time, although growth under full TetA expression is still possible. Contrastingly, further acquisition of *acrR* mutations by *tetR* mutants resulted in much higher gains in both steady-state and dynamical resistance, corroborating the hypothesis that mutations that improve tetracycline efflux provide higher gains in resistance.

To understand how sudden drug exposures can select for loss of TetR repression, we considered a dynamical model of drug responses, which accounts for regulation of expression of resistance and drug action on cell metabolism. Our model describes the accumulation of intracellular tetracycline and expression levels of TetA and TetR, closely following a previously established model that includes the proteome allocation mechanism necessary for growth-dependent gene expression (methods, SI). In this model, loss of TetR regulation is model by simply reducing TetR expression to zero. For both the presence and absence of TetR regulation, we simulated the model in a range of external tetracycline concentrations (Fig. 4C). To compare the two regulatory strategies, we calculated costs associated with the decrease in cell growth following the response and with the burden of unnecessary TetA production. Since the fitness cost of TetA is difficult to determine, we considered scenarios where constitutive TetA expression has different relative contributions to the overall cost of the response. We then calculated how the concentration of tetracycline exposure and relative cost of TetA affect the overall cost of the drug response, thereby determining the optimal regulatory strategy. We found that regardless of the burden associated with TetA expression, regulated TetA expression is preferred during exposures to lower drug concentrations and constitutive TetA expression is preferred at higher drug concentrations. In scenarios where the relative cost of TetA is higher, the threshold drug concentration at which constitutive expression starts being preferred is also higher. Therefore, the influx of drug into the cell can outpace expression of resistance during exposure to high drug concentrations, not allowing the cell enough time to respond. In such situations, constitutive expression of resistance is preferred despite the potential costs associated with unnecessary expression.

Mobile elements as a general strategy of mutating regulatory pathways.

Both the Steady and Dynamic environments resulted in an abundance of regulatory mutations, and many of these were implemented by the insertion of transposable elements. Crucially, all 3 Dynamic populations evolved independent *IS5* transposon insertions inside the *tetR* gene, making TetA expression constitutive, and all 6 populations featured mutations upregulating AcrB expression, with 4 of those implemented by transposon insertions. Additionally, populations in both environments also featured high-abundance mutations in porin regulator *ompR* and in the promoter of ribosomal RNA genes. Overall, the most dominant mutations we observed throughout the experiment included several examples of the disruption of transcription repressors and of their binding sites, with about half of mutations mediated by transposon insertions. Additionally, transposon insertions also introduced an additional promoter for *acrB* in population St-1 and the large deletion of chemotaxis and motility genes in population Dyn-2 was mediated by a copy of transposable element *IS1* flanking the region. Populations in both environments also exhibited a wealth of mutations in genes related to mobile genetic elements that, although not among the most dominant, were present in detectable levels. We obtained comparatively much fewer mutations in non-regulatory genes (*acrB, rpoB* and *plsB*), and these mutations only appeared later in the experiment in lineages that already possessed regulatory mutations. The *acrB* mutations that conferred the highest tetracycline resistance only emerged in steady environments. Therefore, these results support the notion that microbial evolution in new environments proceeds first through regulatory mutations, which are more accessible than low-probability mutations to reach optimal phenotypes.

Discussion

Bacteria often occupy niches where conditions change quickly[1–4]. While the evolution of new features or the repurposing of existing ones leads to genotypes that are highly optimized for the new environment, this evolution might depend on rare mutations and may not be achieved soon enough[24,25]. Therefore, the initial evolution of microbes in hostile environments is dominated by mutations that are more readily accessible, such as the disruption of repression to achieve the upregulation of relevant genes[28–31,52,53]. Here, we determined the role of the dynamics of the environment in the evolution of antibiotic responses. We found that steady environments where drug concentrations do not change so quickly led to the evolution of the AcrB efflux pump through point mutations that optimize it to tetracycline[40,41]. Meanwhile, dynamic environments where drug concentrations change quickly did not result in such refinement of protein function, but instead led to the abolishment of regulation of the *tet* operon, the main resistance mechanism against tetracycline. These experiments show that the dynamics of the environment dictate the evolution of cell responses. In future work, it will be interesting to further characterize the effects of dynamics on evolution, such as if dynamic regimens with lower concentrations might ease evolutionary bottlenecks, or if longer periods in the absence of drug might reduce the benefits of constitutive expression of resistance.

In both environments, evolution proceeded first through regulatory mutations, with a high prevalence of transposon insertions. Previous work shows that exposure to low levels of

tetracycline results in high levels of mobile element activity via the sensing of cellular stress[54,55]. Evolution under high drug levels requires quick adaptation, and transposon insertions provide a quick way of upregulating useful genes, either by disrupting repressors or inserting new promoters, or also deleting harmful genes. Transposon insertions also offer the advantage of being reversible[51,53]. The overwhelming presence of transposon insertions rewiring the regulation of resistance genes, as well as mutations in genes regulating and operating transposable elements, suggests an important role of this mechanism in the short-term evolution of microbes in challenging environments, which is often missed in whole-genome sequencing analysis[52,56,57].

The sudden drug exposures during antibiotic treatments are likely to play a role in the evolution of pathogens in clinical environments. While the *tet* operon provides relatively fast responses to tetracycline, many other resistance mechanisms are induced only by downstream effects of the drug and respond much more slowly[58,59]. Constitutive expression of resistance would be even more beneficial in these cases. Indeed, loss-of-function mutations in transcription repressors of resistance genes are often found in clinical isolates. Our results suggest that these mutations can serve both the purpose of bypassing the induction of drug responses in the adaptation to sudden antibiotic exposures and the purpose of de-repressing less optimal resistance mechanisms that are not sufficiently activated by the drug.

Methods

Media, drugs, and strains. All experiments were conducted in M63 minimal medium (2g/l (NH4)2SO4, 13.6g/l KH2PO4, 0.5mg/l FeSO4,7H2O) supplemented with 0.2% glucose, 0.01% casamino acids, 1mM MgSO4 and 1.5mM thiamine. Tetracycline and IPTG solutions were freshly made from powder stocks (Sigma) and filter-sterilized before each experiment. As the ancestral strain, we used *E. coli* K-12 strain MG1655 *rph*+ Δ*LacIZYA*, with the native *tet* resistance mechanism from the Tn*10* transposon integrated in the chromosome at site HKO22 with a pIT3-CH integrating plasmid.

Setup of continuous cultures. Glass vials were coated with Sigmacote (Sigma) to prevent biofilm growth. Vials, vial heads, tubing, and all connections were autoclaved before assembly. Complete sterilization was ensured by running 10% bleach, 70% ethanol, and sterile water consecutively through all tubing. Experiments were carried out at 37 °C in sterile M63 media (as described above). Drug media consisted of M63 media with tetracycline added to 1000 µg/ml, mixed until completely dissolved in solution, and filter sterilized into the container used for the experiment. Vials were filled with 15 ml of M63 and used to blank OD measurements.

Regimens of drug administration. The experiment consisted of two experimental groups (dynamic and steady); each group was composed of three replicate vials. Samples were taken daily and stored as glycerol stocks in a 96 well plate at -80 °C. Vials were switched daily to prevent biofilm growth.

The steady group was run as a morbidostat, where cultures were delivered a fixed volume of media every five minutes with a dilution rate of 0.35 h^{-1}. In cycles where the OD was

above a threshold of 0.15 and OD increased over the previous 30 minutes, a 4.4 µg/ µL dose of tetracycline was also delivered.

The dynamic group was run as a modified turbidostat, where culture density was maintained at a target of 0.15 OD by dilution at a variable rate with drug free M63, delivered every five minutes. A large dosage spike of tetracycline was delivered every 24 hours, unless cultures had not yet recovered from the previous drug exposure. Cultures were diluted to half of the target OD by the addition of media with drug to the desired concentration. Once cultures recovered to the threshold OD, turbidostat control was resumed and maintained until the following dosage spike. The dosage was increased by a factor of $1/(5 - t_r)$ for the following exposure, where t_r is the recovery time in hours.

Genomic sequencing of evolved populations. Glycerol stocks from the final evolved populations were inoculated 1:100 in 5 ml LB and grown for five hours. Samples were pelleted and DNA was extracted using DNEasy Kits (Qiagen). Genomic sequencing was performed by the Genomics and Molecular Biology Shared Resource, and sequencing analysis was carried out by the Data Analytics core at Dartmouth.

Genotyping of isolates. The presence of selected SNPs in isolates was confirmed via Sanger sequencing. Glycerol stock samples for each population for each day were inoculated 1:100 in LB and grown for 2 hours, then streaked on LB agar plates and grown at 37 °C overnight. 10 individual colonies from each sample were picked, selected genomic regions were PCR amplified and cleaned (Qiagen) and sent for sequencing to the Dartmouth College Genomics and Molecular Biology Shared Resources Core. Isolates known to have SNPs were preserved as glycerol stocks at -80 °C. For samples with transposon insertions, the PCR product was assessed by gel electrophoresis to confirm insertions.

Plate reader experiments. Glycerol stock of relevant samples were inoculated into M63 or LB media and grown overnight. Each strain was inoculated 1:1000 in M63 and exposed to a gradient of 12 tetracycline concentrations (100-1000 µg/ml) during early log phase. Experiments were carried out at 37 °C in a Synergy Neo2 plate reader (BioTek). We measured both the time until one doubling was achieved following exposure and the steady-state growth rate after recovery. We extract from this assay two complementary measures of resistance: 1) *Dynamical Resistance,* which is the drug concentration that introduces a 2-hour delay in the time to reach one doubling following drug exposure in comparison to the absence of drug, and 2) *Steady-State Resistance*, which is the drug concentration that halves the growth rate of the recovered population (similar to the IC_{50} concentration).

Mathematical Model. We model the main biochemical interactions involved in the response as a set of differential equations that describe changes in the concentrations of the intracellular drug (d), the efflux pump TetA (a), and the repressor protein TetR (r):

$$\dot{d} = K_i\big(D(t) - d_f\big) - \frac{K_a a d_f}{k_a + d_f} - \lambda d$$

$$\dot{a} = f\, H_a\big(r_f\big) - \lambda a$$

$$\dot{r} = f\ H_r(r_f) - \lambda r$$

where K_i stands for the import rate, D for extracellular drug concentration, d_f for free intracellular drug, K_a for the catalytic rate constant of TetA, k_a the Michaelis constant, respectively, r_f free repressor, and $H_a(r_f)$ and $H_r(r_f)$ the synthesis rates for TetA and TetR that depend on free TetR. To simulate loss of TetR function, we set $H_r(r_f) = 0$. Since the biochemical binding and unbinding of the substrate to the transcription factor typically happens at a much faster rate than the aforementioned processes, we consider their unbound (free) forms (d_f, r_f) to be in chemical equilibrium with the bound form $[rd]$ with a dissociation constant K_d, such that $r_f d_f = [rd]$. The term $K_i(D(t) - d_f)$ represents the diffusion of drug across the membrane into the cell, $\frac{K_a a d_f}{(k_a + d_f)}$ the export of drug out of the cell by the efflux pump. The terms λd, λa and λr represent the dilution due to cell growth of drug, TetA and TetR, respectively, where λ is the current growth rate. Both f, which allows us to modulate the strength of gene expression, and the growth rate λ depend on the nutrient level and the intracellular drug concentration.

To model these dependencies, we used the framework introduced by Scott et al. In this framework κ_n and κ_t are the nutritional and translational capacity of the cell, respectively. Here, we refer to their base values (full nutrients, no drug) as κ_n^0 and κ_t^0, respectively.

For the nutritional capacity, we assume a Monod dependency on the limiting nutrient concentration c with $\kappa_n = \kappa_n^0 \frac{c}{c_0 + c}$, where c_0 is the half-maximum concentration, which we assume to be much smaller than the nutrient concentration at the top of the trap in order to obtain the sharp growth boundary. For the translational capacity, we assume inhibition by tetracycline according to $\kappa_t = \kappa_t^0 \frac{K_{ribo}}{K_{ribo} + d_f}$, where the fraction represents the fraction of free ribosomes in the cell, and K_{ribo} is the dissociation constant for tetracycline and the ribosome. Lower K_{ribo} values correspond to stronger inhibition, and vice versa. According to (Scott et al. 2010), the growth rate can then be calculated as $\lambda = \frac{\phi_c}{\rho} \cdot \frac{\kappa_t \kappa_n}{\kappa_t + \kappa_n}$, where $\phi_c = 0.48$ and $\rho = 0.76$ are universal constants.

κ_t^0 has a universal value of $4.5\ h^{-1}$for *E. coli*. κ_n^0 varies according to nutrient quality. We chose $\kappa_n^0 = 7.176\ h^{-1}$ such that $\lambda_0 = \frac{\phi_c}{\rho} \cdot \frac{\kappa_t^0 \kappa_n^0}{\kappa_t^0 + \kappa_n^0}$ (corresponding to a state without tetracycline, at full nutrients) yields a maximum growth rate of $\lambda_0 = 0.029\ min^{-1}$ as observed in the experiment.

We assume that TetA and TetR are part of the P sector of the proteome, which scales as $\phi_P = \phi_c \cdot \frac{\kappa_t}{\kappa_t + \kappa_n}$. Without regulation of the synthesis rates $H_a(r_f)$ and $H_r(r_f)$, we would expect the concentrations of TetA and TetR to scale in the same way. Hence, we define $f = \frac{\lambda}{\lambda_0} \cdot \frac{\kappa_t}{\kappa_t + \kappa_n} / \frac{\kappa_t^0}{\kappa_t^0 + \kappa_n^0}$, which leads to steady states proportional to $\sim \frac{\kappa_t}{\kappa_t + \kappa_n}$ and simplifies to $f = 1$ at full nutrients and no drug.

Remaining model parameters: $K_i = 0.015\, min^{-1}$, $K_a = 50\, min^{-1}$, $k_a = 10\ \mu M$,$K_d = 0.001\ \mu M$, $K_{ribo} = 1\ \mu M$, $H_a(r_f) = A\frac{r_{0,a}^5}{r_{0,a}^5+r_f^5}$, $A = 0.008\ \mu M/min$, $r_{0,a} = 0.0001\ \mu M$, $H_r(r_f) = R\frac{r_{0,r}^3}{r_{0,r}^3+r_f^3}$, $R = 0.0003\ \mu M min^{-1}$, $r_{0,a} = 0.000075\ \mu M$, $D(t) = 0\ or\ 50 \mu M$, $D_n = 1200\ \mu m^2/min$, $\gamma_0 = 0.4\ a.u.\,\mu m^{-2} min^{-1}$, $c_0 = 0.01\ a.u.\,\mu m^{-2}$

Conflict of Interest

The authors declare that the research was conducted in the absence of any commercial or financial relationships that could be construed as a potential conflict of interest.

Author Contributions

D.S. and J.C. designed the study. J.C. performed the experiments. All authors analyzed the data. D.S. and H.G. designed the mathematical model. All authors wrote the manuscript.

Funding

D.S. is supported by a grant from the NIH/NIGMS P20 GM130454-02.

Acknowledgements

Genomic sequencing was carried out in the Genomics and Molecular Biology Shared Resource at Dartmouth, which is supported by NCI Cancer Center Support Grant 5P30CA023108 and NIH 1S10OD030242 awards. Analysis of sequencing data was performed by the Data Analytics Core through the Dartmouth Center for Quantitative Biology with support from NIGMS P20GM130454 and NIH S10OD025235 awards.

References

1. Wani, A. K., Akhtar, N., Sher, F., Navarrete, A. A. & Américo-Pinheiro, J. H. P. Microbial adaptation to different environmental conditions: molecular perspective of evolved genetic and cellular systems. *Archives of Microbiology* vol. **204** (2022).
2. Scheuerl, T. *et al.* Bacterial adaptation is constrained in complex communities. *Nat Commun* **11**, (2020).
3. Lopatkin, A. J. *et al.* Antibiotics as a selective driver for conjugation dynamics. *Nat Microbiol* **1**, (2016).

4. Baym, M. *et al.* Spatiotemporal microbial evolution on antibiotic landscapes. *Science (1979)* **353**, (2016).

5. Arnoldini, M., Mostowy, R., Bonhoeffer, S. & Ackermann, M. Evolution of Stress Response in the Face of Unreliable Environmental Signals. *PLoS Comput Biol* **8**, (2012).

6. Logue, J. B., Findlay, S. E. G. & Comte, J. Editorial: Microbial responses to environmental changes. *Frontiers in Microbiology* vol. **6** (2015).

7. Mougi, A. Eco-evolutionary dynamics in microbial interactions. *Sci Rep* **13**, (2023).

8. Dekel, E. & Alon, U. Optimality and evolutionary tuning of the expression level of a protein. *Nature* **436**, 588–592 (2005).

9. Zorraquino, V., Kim, M., Rai, N. & Tagkopoulos, I. The genetic and transcriptional basis of short and long term adaptation across multiple stresses in Escherichia coli. *Mol Biol Evol* **34**, 707–717 (2017).

10. Schultz, D., Palmer, A. C. & Kishony, R. Regulatory Dynamics Determine Cell Fate following Abrupt Antibiotic Exposure. *Cell Syst* **5**, 509-517.e3 (2017).

11. Patel, V. & Matange, N. Adaptation and compensation in a bacterial gene regulatory network evolving under antibiotic selection. *eLife* **10**, e70931 (2021).

12. Band, V. I. & Weiss, D. S. Heteroresistance: A cause of unexplained antibiotic treatment failure? *PLoS Pathog* **15**, 1–7 (2019).

13. Sánchez-Romero, M. A. & Casadesús, J. Contribution of phenotypic heterogeneity to adaptive antibiotic resistance. *Proc Natl Acad Sci U S A* **111**, 355–360 (2014).

14. García, M. S. Early antibiotic treatment failure. *Int J Antimicrob Agents* **34**, 14–19 (2009).

15. Han, B. *et al.* The source, fate and prospect of antibiotic resistance genes in soil: A review. *Frontiers in Microbiology* vol. **13** (2022).

16. Drlica, K. The mutant selection window and antimicrobial resistance. *Journal of Antimicrobial Chemotherapy* vol. **52** 11–17 (2003).

17. Stanton, I. C., Murray, A. K., Zhang, L., Snape, J. & Gaze, W. H. Evolution of antibiotic resistance at low antibiotic concentrations including selection below the minimal selective concentration. *Commun Biol* **3**, (2020).

18. Wright, G. D. Environmental and clinical antibiotic resistomes, same only different. *Curr Opin Microbiol* **51**, 57–63 (2019).

19. Windels, E. M. *et al.* Bacterial persistence promotes the evolution of antibiotic resistance by increasing survival and mutation rates. *ISME Journal* **13**, 1239–1251 (2019).

20. Balaban, N. Q. *et al.* Definitions and guidelines for research on antibiotic persistence. *Nat Rev Microbiol* **17**, 441–448 (2019).

21. Windels, E. M., Van Den Bergh, B. & Michiels, J. Bacteria under antibiotic attack: Different strategies for evolutionary adaptation. *PLoS Pathog* **16**, (2020).

22. Sulaiman, J. E. & Lam, H. Evolution of Bacterial Tolerance Under Antibiotic Treatment and Its Implications on the Development of Resistance. *Frontiers in Microbiology* vol. **12** (2021).

23. Olofsson, S. K. & Cars, O. Optimizing drug exposure to minimize selection of antibiotic resistance. in *Clinical Infectious Diseases* vol. **45** (2007).

24. Mahrt, N. *et al.* Bottleneck size and selection level reproducibly impact evolution of antibiotic resistance. *Nat Ecol Evol* **5**, 1233–1242 (2021).

25. Ghaddar, N., Hashemidahaj, M. & Findlay, B. L. Access to high-impact mutations constrains the evolution of antibiotic resistance in soft agar. *Sci Rep* **8**, (2018).

26. Blair, J. M. A., Webber, M. A., Baylay, A. J., Ogbolu, D. O. & Piddock, L. J. V. Molecular mechanisms of antibiotic resistance. *Nat Rev Microbiol* **13**, 42–51 (2014).

27. Lozada-Chávez, I., Janga, S. C. & Collado-Vides, J. Bacterial regulatory networks are extremely flexible in evolution. *Nucleic Acids Res* **34**, 3434–3445 (2006).

28. Grekov, I., Thöming, J. G., Kordes, A. & Häussler, S. Evolution of *Pseudomonas aeruginosa* toward higher fitness under standard laboratory conditions. *ISME Journal* **15**, 1165–1177 (2021).

29. Lind, P. A., Farr, A. D. & Rainey, P. B. Experimental evolution reveals hidden diversityin evolutionary pathways. *eLife* **4**, e07074–e07074 (2015).

30. Marvig, R. L., Sommer, L. M., Molin, S. & Johansen, H. K. Convergent evolution and adaptation of *Pseudomonas aeruginosa* within patients with cystic fibrosis. *Nat Genet* **47**, 57–64 (2015).

31. Prud'homme, B., Gompel, N. & Carroll, S. B. Emerging principles of regulatory evolution. *In the Light of Evolution* **1**, 109–127 (2007).

32. de Cristóbal, R. E., Vincent, P. A. & Salomón, R. A. Multidrug resistance pump AcrAB-TolC is required for high-level, Tet(A)-mediated tetracycline resistance in Escherichia coli. *Journal of Antimicrobial Chemotherapy* **58**, 31–36 (2006).

33. Fernández, L. & Hancock, R. E. W. Adaptive and Mutational Resistance: Role of Porins and Efflux Pumps in Drug Resistance. *Clin. Microbiol. Rev.* **25**, 661–681 (2012).

34. Webber, M. A. & Piddock, L. J. V. The importance of efflux pumps in bacterial antibiotic resistance. *Journal of Antimicrobial Chemotherapy* **51**, 9–11 (2003).

35. Lederer, T., Takahashi, M. & Hillen, W. Thermodynamic Analysis of Tetracycline-Mediated Induction of Tet Repressor by a Quantitative Methylation Protection Assay. *Anal Biochem* **232**, 190–196 (1995).

36. Ramos, J. L. *et al.* The TetR Family of Transcriptional Repressors. *Microbiology and Molecular Biology Reviews* **69**, 326–356 (2005).

37. Su, C. C., Rutherford, D. J. & Yu, E. W. Characterization of the multidrug efflux regulator AcrR from Escherichia coli. *Biochem Biophys Res Commun* **361**, 85–90 (2007).

38. Nguyen, T. N. M., Phan, Q. G., Duong, L. P., Bertrand, K. P. & Lenski, R. E. Effects of carriage and expression of the Tn10 tetracycline-resistance operon on the fitness of Escherichia coli K12. *Mol Biol Evol* **6**, (1989).

39. Eckert, B. & Beck, C. F. Overproduction of Transposon Tn10-Encoded Tetracycline Resistance Protein Results in Cell Death and Loss of Membrane Potential. *J Bacteriol* **171**, 3557–3559 (1989).

40. Blair, J. M. A. *et al.* AcrB drug-binding pocket substitution confers clinically relevant resistance and altered substrate specificity. *Proc Natl Acad Sci* **112**, 3511–3516 (2015).

41. Hoeksema, M., Jonker, M. J., Brul, S. & Ter Kuile, B. H. Effects of a previously selected antibiotic resistance on mutations acquired during development of a second resistance in Escherichia coli. *BMC Genomics* **20**, (2019).

42. Reuter, A. *et al.* Direct visualisation of drug-efflux in live Escherichia coli cells. *FEMS Microbiol Rev* **44**, 782–792 (2020).

43. Toprak, E. *et al.* Evolutionary paths to antibiotic resistance under dynamically sustained drug selection. *Nat Genet* **44**, 101–105 (2012).

44. Toprak, E. *et al.* Building a morbidostat: An automated continuous-culture device for studying bacterial drug resistance under dynamically sustained drug inhibition. *Nat Protoc* **8**, 555–567 (2013).

45. Jansen, G., Barbosa, C. & Schulenburg, H. Experimental evolution as an efficient tool to dissect adaptive paths to antibiotic resistance. *Drug Resistance Updates* **16**, 96–107 (2013).

46. Reading, E. *et al.* Perturbed structural dynamics underlie inhibition and altered efflux of the multidrug resistance pump AcrB. *Nat Commun* **11**, (2020).

47. Ornik-Cha, A. *et al.* Structural and functional analysis of the promiscuous AcrB and AdeB efflux pumps suggests different drug binding mechanisms. *Nat Commun* **12**, (2021).

48. Spoering, A. L., Vulić, M. & Lewis, K. GlpD and PlsB participate in persister cell formation in Escherichia coli. *J Bacteriol* **188**, 5136–5144 (2006).

49. Knopp, M. & Andersson, D. I. Amelioration of the fitness costs of antibiotic resistance due to reduced outer membrane permeability by upregulation of alternative porins. *Mol Biol Evol* **32**, 3252–3263 (2015).

50. Hinton, D. M. & Musso, R. E. Specific in vitro transcription of the insertion sequence IS2. *J. Mol. Biol.* **169**, 53–81 (1983).

51. Siguier, P., Gourbeyre, E. & Chandler, M. Bacterial insertion sequences: Their genomic impact and diversity. *FEMS Microbiol Rev* **38**, 865–891 (2014).

52. Fan, C. *et al.* Defensive Function of Transposable Elements in Bacteria. *ACS Synth Biol* **8**, 2141–2151 (2019).

53. Vandecraen, J., Chandler, M., Aertsen, A. & Van Houdt, R. The impact of insertion sequences on bacterial genome plasticity and adaptability. *Critical Reviews in Microbiology* vol. **43** 709–730 (2017).

54. Cornforth, D. M. & Foster, K. R. Competition sensing: The social side of bacterial stress responses. *Nature Reviews Microbiology* vol. **11** 285–293 (2013).

55. Stevens, A. M., Shoemaker, N. B., Li, L.-Y. & Salyers, A. A. *Tetracycline Regulation of Genes on Bacteroides Conjugative Transposons*. *Journal of Bacteriology* vol. **175** (1993).

56. Nagy, Z. & Chandler, M. Regulation of transposition in bacteria. *Res Microbiol* **155**, 387–398 (2004).

57. Walker, B. J. *et al.* Pilon: An integrated tool for comprehensive microbial variant detection and genome assembly improvement. *PLoS One* **9**, (2014).

58. Grkovic, S., Brown, M. H. & Skurray, R. A. Transcriptional regulation of multidrug efflux pumps in bacteria. *Semin Cell Dev Biol* **12**, 225–237 (2001).

59. Depardieu, F., Podglajen, I., Leclercq, R., Collatz, E. & Courvalin, P. Modes and Modulations of Antibiotic Resistance Gene Expression. *Clin. Microbiol. Rev.* **20**, 79–114 (2007).

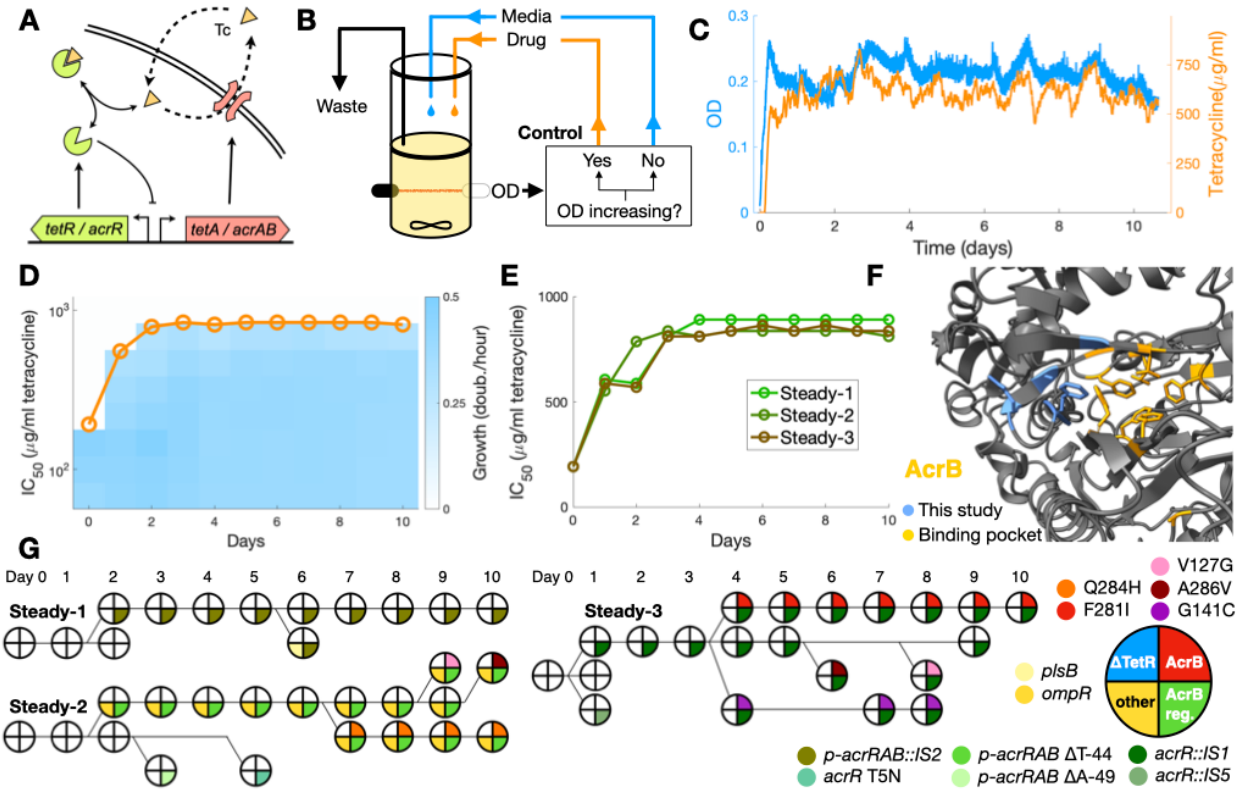

Figure 1. Steady drug regimens result in mutations in the AcrB binding pocket. A. *tet* and *acr* resistance mechanisms: tetracycline (Tc), a translation inhibitor, diffuses across the cell membrane and binds transcription repressors TetR and AcrR, which become inactive and release expression of efflux pumps TetA and AcrAB, which export tetracycline out of the cell. **B.** Continuous culture setup with media and drug control for the Steady environment. If OD increased over the previous half hour, a fixed drug dose is added to the culture. **C.** Progression of OD and drug concentration for population Steady-2 over the course of the experiment. **D.** Growth rates of samples of population Steady-2 from each day. Circles indicate drug concentrations at which growth is reduced to half (IC_{50} concentration). **E.** Progression of resistance for each Steady population, measured by the IC_{50} concentration. **F.** Locations of AcrB mutations in evolved strains within the protein structure. We found several mutations around the protein binding site. **G.** Phylogenetic trees of mutants in each Steady population. 5 isolates were picked from each population from each day, and presence of select mutations was confirmed by sequencing. Phylogenetic relationships were inferred from the co-occurrence of each mutation in each isolate. Lineages were plotted in the days in which they were detected in our sampling.

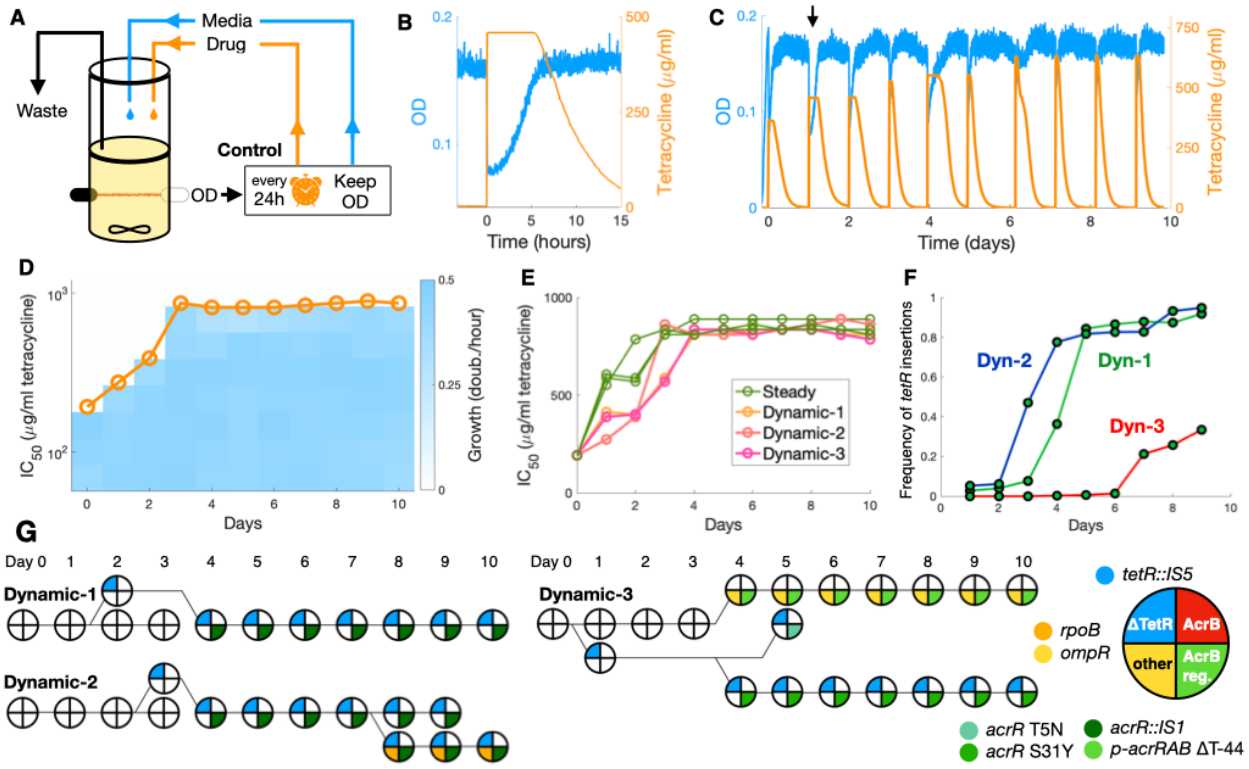

Figure 2. Dynamic drug regimens result in transposon insertions in the *tetR* gene. **A.** Continuous culture setup with media and drug control for the Dynamic environment. Cultures are suddenly exposed to a large drug dose every 24 hours but are otherwise maintained at a target OD by dilution with fresh medium. **B.** Cultures are exposed to tetracycline by the addition of medium containing the drug, reducing OD to half. Dilution with fresh medium resumes when the population doubles to the target OD. **C.** Progression of OD and drug concentration for population Dynamic-2 over the course of the experiment. Arrow indicates the exposure depicted in (B). **D.** Growth rates of samples of population Dynamic-2 from each day. Circles indicate drug concentrations at which growth is reduced to half (IC_{50} concentration). **E.** Progression of resistance for each population, measured by the IC_{50} concentration. Acquisition of resistance is slower in Dynamic populations. **F.** Prevalence of transposon insertions in TetR over time in each Dynamic population. Such mutations were the first to be observed in all Dynamic populations. **G.** Phylogenetic trees of mutants in each Dynamic population. 5 isolates were picked from each population from each day, and presence of select mutations was confirmed by sequencing. Phylogenetic relationships were inferred from the co-occurrence of each mutation in each isolate. Lineages were plotted in the days in which they were detected in our sampling.

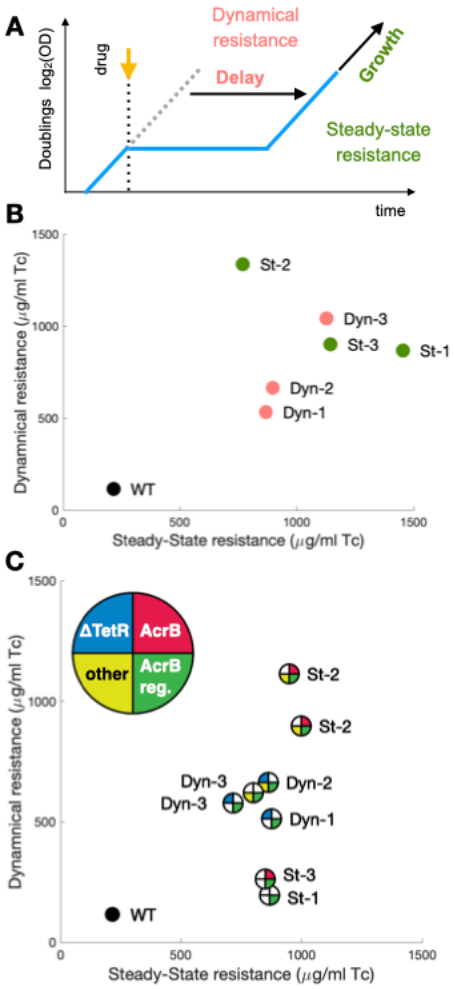

Figure 3. Mutations optimizing *acrB* provide highest resistance and shortest recoveries. A. In experiments with liquid cultures exposed to a step increase in drug concentration, we measure *Dynamical Resistance,* the population-level performance during the transient following exposure, by calculating the delay in the time taken to reach one doubling that is introduced by the addition of drug during mid-log phase. *Steady-state Resistance*, the performance in the steady state, is measured by the maximum growth over one doubling at any point after exposure. **B.** Dynamical and Steady-state resistances for the final evolved populations. Populations Dyn-1 and Dyn-2, where TetR transposon insertions were fixed, performed more poorly in both measures. **C.** Dynamical and Steady-state resistances for select mutants. Mutants with optimized AcrB performed best, and even recovered from drug exposure faster than TetR transposon mutants.

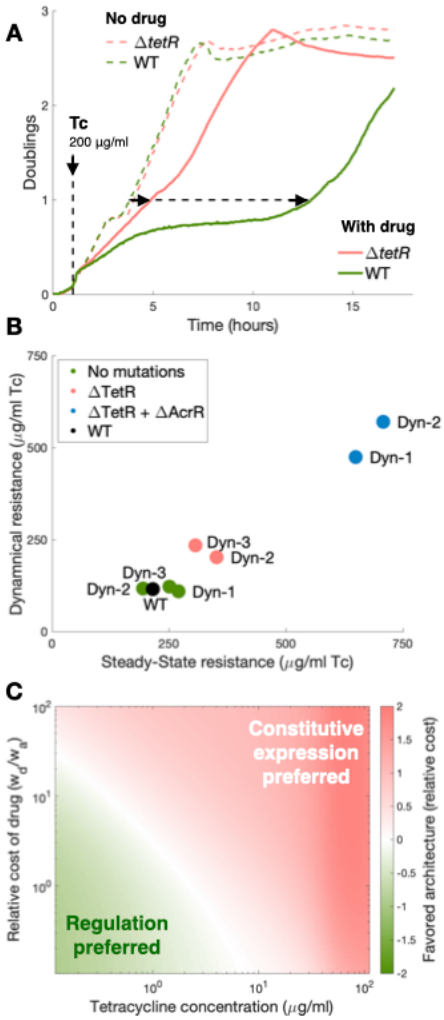

Figure 4. Sudden exposures to high drug doses overwhelm regulated responses. **A.** Growth curves of isolates picked from the same day, one with a transposon insertion in TetR and one without. The vertical dashed line indicates addition of 200 μg/ml tetracycline. The corresponding growth curves under no drug are also included in dashed lines for comparison. The delays for each culture to reache one doubling is indicated. Loss of TetR function reduces the recovery time significantly. **B.** Dynamical and Steady-state resistances for isolates with and without TetR transposon insertions, and also with further regulatory mutations in the *acr* operon. Loss of TetR function provides significant gains in resistance, but further mutations optimizing the *acr* operon provide even larger gains. **C.** We simulate drug responses using a mathematical model tracking intracellular drug concentration. Loss of TetR repression is implemented by setting TetR synthesis rate to zero. We simulated the system with and without TetR repression, during exposures to a range of tetracycline concentrations. To compare the two regulatory strategies, we calculated costs associated with the decrease in cell growth and with the burden of unnecessary TetA production. We considered scenarios where constitutive TetA expression has different relative contributions to the overall cost of the response. Regardless of the relative cost of TetA, constitutive expression is preferred during exposures to high enough drug doses.

Population	Gene	Function	Frequency
Std-1	*p-acrRAB::IS2*	Multidrug efflux pump	0.86
Std-1	*plsB*	Phospholipid biosynthesis, multidrug tolerance	0.63
Std-1	*insB1*	Insertion element IS1 protein	0.15
Std-1	*del cheA/ motAB/flhCD**	Chemotaxis, motility	1
Std-2	*p-acrRAB*	Multidrug efflux pump promoter	0.99
Std-2	*ompR* (R15S)	Porin regulator, osmotic stress	0.97
Std-2	*yhdP*	Phospholipid transport factor	0.37
Std-2	*acrB* (Q284H)	Multidrug efflux pump	0.36
Std-3	*acrR::IS1*	AcrB multidrug efflux pump repressor	0.78
Std-3	*acrB* (F281I)*	Multidrug efflux pump	0.75
Std-3	*p-rrsG* (2729370)	16S ribosomal RNA	0.27
Std-3	*p-rrsG* (2729333)	16S ribosomal RNA	0.24
Std-3	*del cheA/ motAB/flhCD**	Chemotaxis, motility	1

Table 1: Relevant mutations found in evolved Steady populations. Mutations shown are present above a 0.15 frequency and are not detected in the ancestral WT population. *Found in very low abundance in the ancestral WT population.

Population	Gene	Function	Frequency
Dyn-1	*tetR::IS5* (1)	TetA tetracycline efflux pump repressor	0.97
Dyn-1	*acrR::IS1*	AcrB multidrug efflux pump repressor	0.73
Dyn-1	*del cheA/ motAB/flhCD**	Chemotaxis, motility	1
Dyn-2	*tetR::IS5* (2)	TetA tetracycline efflux pump repressor	0.99
Dyn-2	*acrR::IS1*	AcrB multidrug efflux pump repressor	0.66
Dyn-2	*rpoB*	RNA polymerase subunit β	0.52
Dyn-2	*kgtP*	Transporter for α-ketoglutarate	0.20
Dyn-2	*rhsA*	Rearrangement hotspot element	0.18
Dyn-2	*insF1*	Insertion element IS3 transposase	0.15
Dyn-2	*rrfF*	5S ribosomal RNA	0.15
Dyn-2	*del tar/cheAW/ motAB/flhCD**	Chemotaxis, motility	1
Dyn-3	*ompR* (R15S)	Porin regulator, osmotic stress	0.67
Dyn-3	*p-acrRAB*	Multidrug efflux pump promoter	0.61
Dyn-3	*intK*	Prophage, drug resistance	0.30
Dyn-3	*tetR::IS5* (3)	TetA tetracycline efflux pump repressor	0.27
Dyn-3	*flu*	Prophage, self-recognizing antigen	0.23
Dyn-3	*acrR* (S31Y)	AcrB multidrug efflux pump repressor	0.23
Dyn-3	*rhsB*	Rearrangement hotspot element	0.20
Dyn-3	*insL1*	Insertion element IS186 transposase	0.19
Dyn-3	*trmA*	tRNA methyltransferase	0.15

Table 2: Relevant mutations found in evolved Dynamic populations. Mutations shown are present above a 0.15 frequency and are not detected in the ancestral WT population. *Found in very low abundance in the ancestral WT population.

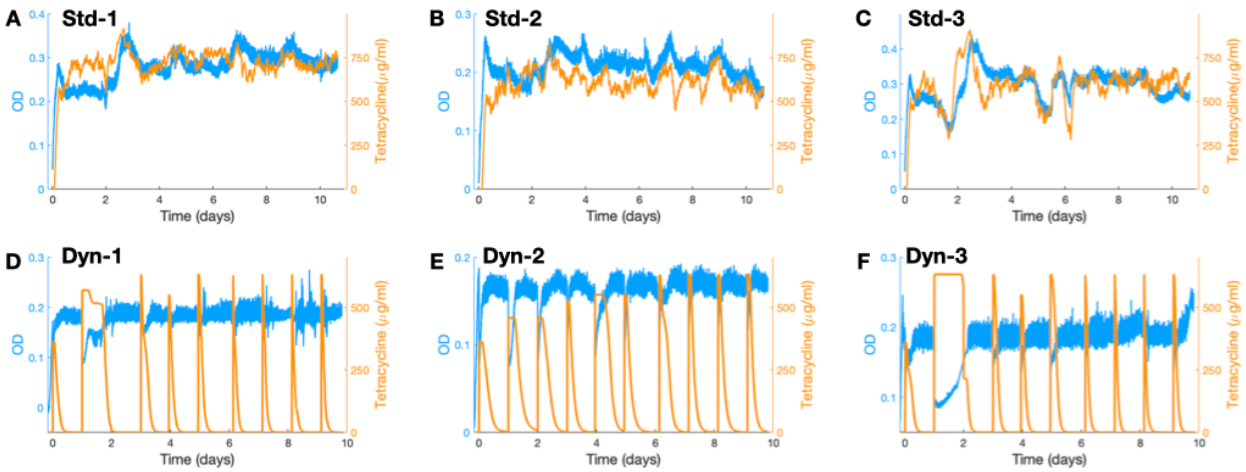

Figure S1. OD and tetracycline concentration over the course of the experiment. Optical densities and tetracycline concentrations measured over time for **A-C** Steady populations and **D-F** Dynamic populations. Populations Dyn-1 and Dyn-2 recovered slowly from the second exposure and skipped the third exposure.

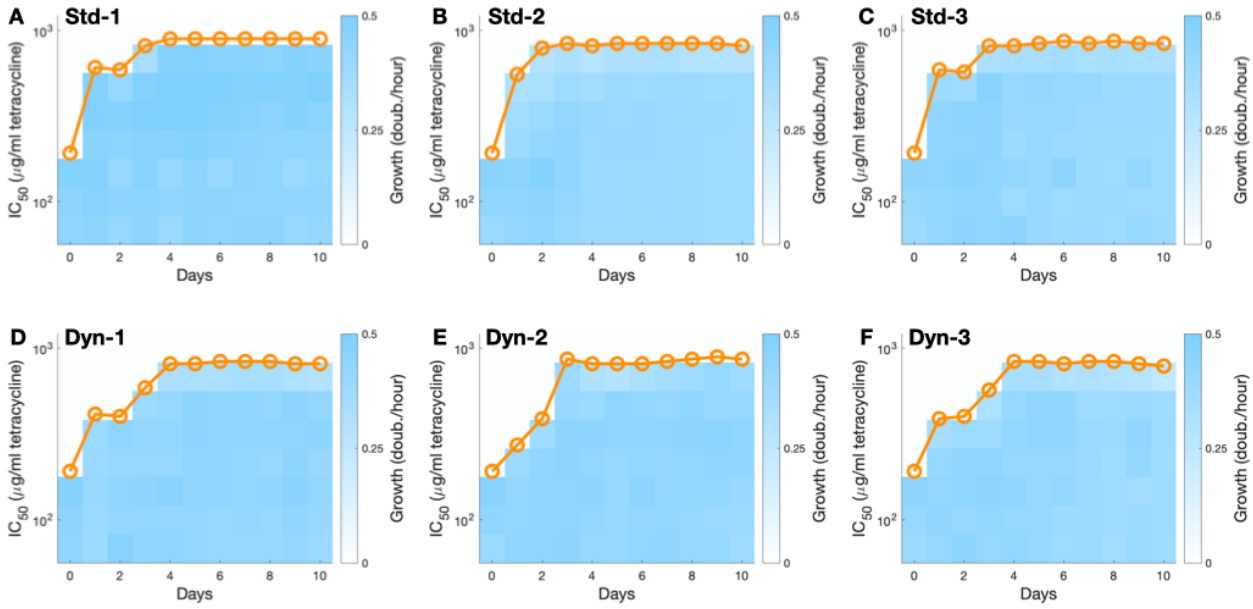

Figure S2. Progression of tetracycline resistance in each population. A-F. Samples from each population in each day were grown in tetracycline concentrations picked from a gradient and growth rates were determined in each case. Circles indicate the drug concentration at which growth is reduced to half (IC_{50} concentration).

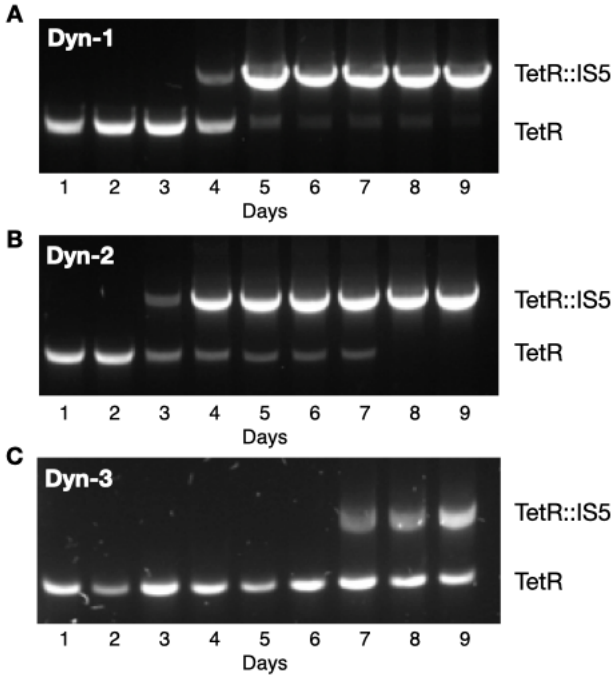

Figure S3. Prevalence of *IS5* insertions in the *tetR* gene over the course of the experiment. PCR amplification of the *tet* operon showing acquisition of transposon insertion in each Dynamic population. We quantified the relative intensity of the bands to estimate the prevalence of TetR transposon insertions in each population in each day.

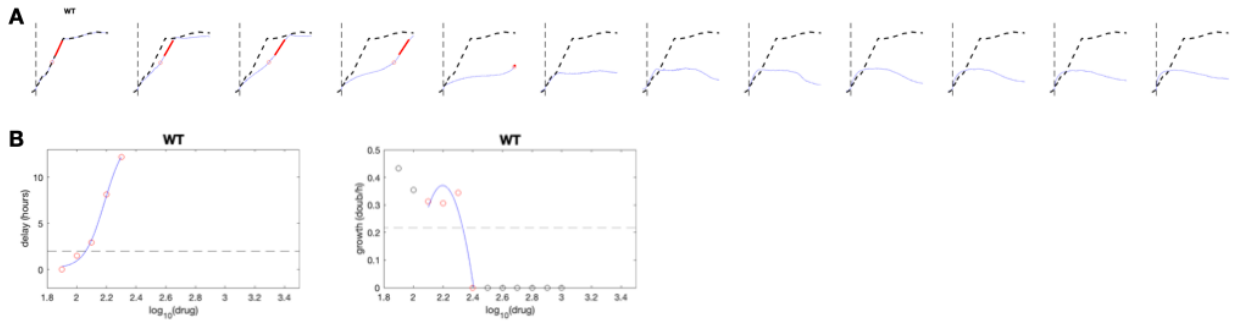

Figure S4. Calculation of steady-state and dynamical resistances for the WT ancestral strain. A. Growth curves of the WT ancestral strain. Plots are $\log_2$(OD) over 20 hours. Vertical dashed line indicates addition of tetracycline picked from a gradient of zero in the first column then 100 to 1000 µg/ml in columns 2 to 12. The corresponding growth curve with zero drug is included in a dashed line for comparison. The point at which the culture reaches a doubling is indicated, as well as the linear fit during steady-state growth following recovery. **B.** Dynamic resistance is calculated as the drug concentration that causes a 2-hour delay in the time to reach one doubling following drug exposure. Steady-state resistance is calculated as the drug concentration that reduces steady-state growth to half of the growth rate under no drug. Curves were fit with second order polynomials.

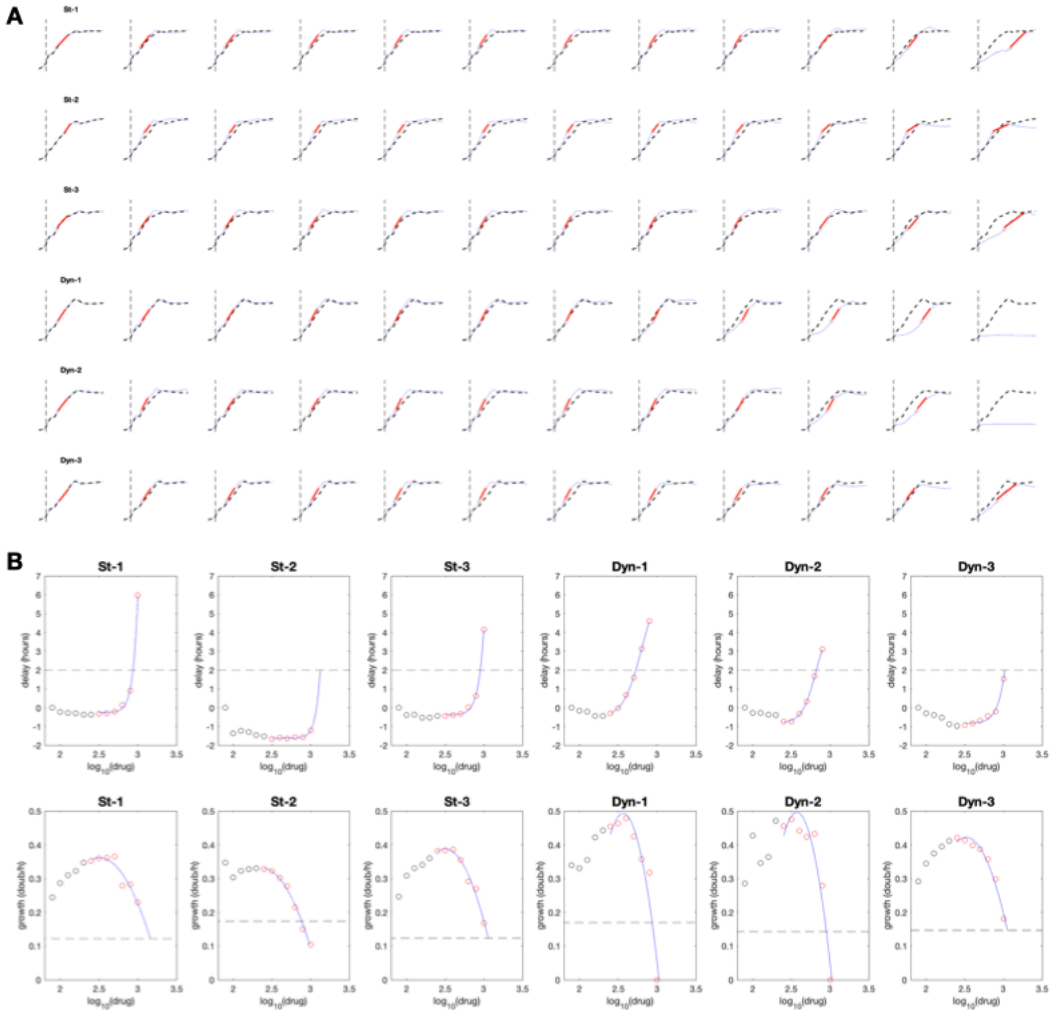

Figure S5. Calculation of steady-state and dynamical resistances for final evolved populations. A. Growth curves of the final populations. Plots are $\log_2$(OD) over 20 hours. Vertical dashed line indicates addition of tetracycline picked from a gradient of zero in the first column then 100 to 1000 µg/ml in columns 2 to 12. The corresponding growth curve with zero drug is included in a dashed line for comparison. The point at which the culture reaches a doubling is indicated, as well as the linear fit during steady-state growth following recovery. **B.** Dynamic resistance is calculated as the drug concentration that causes a 2-hour delay in the time to reach one doubling following drug exposure. Steady-state resistance is calculated as the drug concentration that reduces steady-state growth to half of the growth rate under no drug. Curves were fit with second order polynomials.

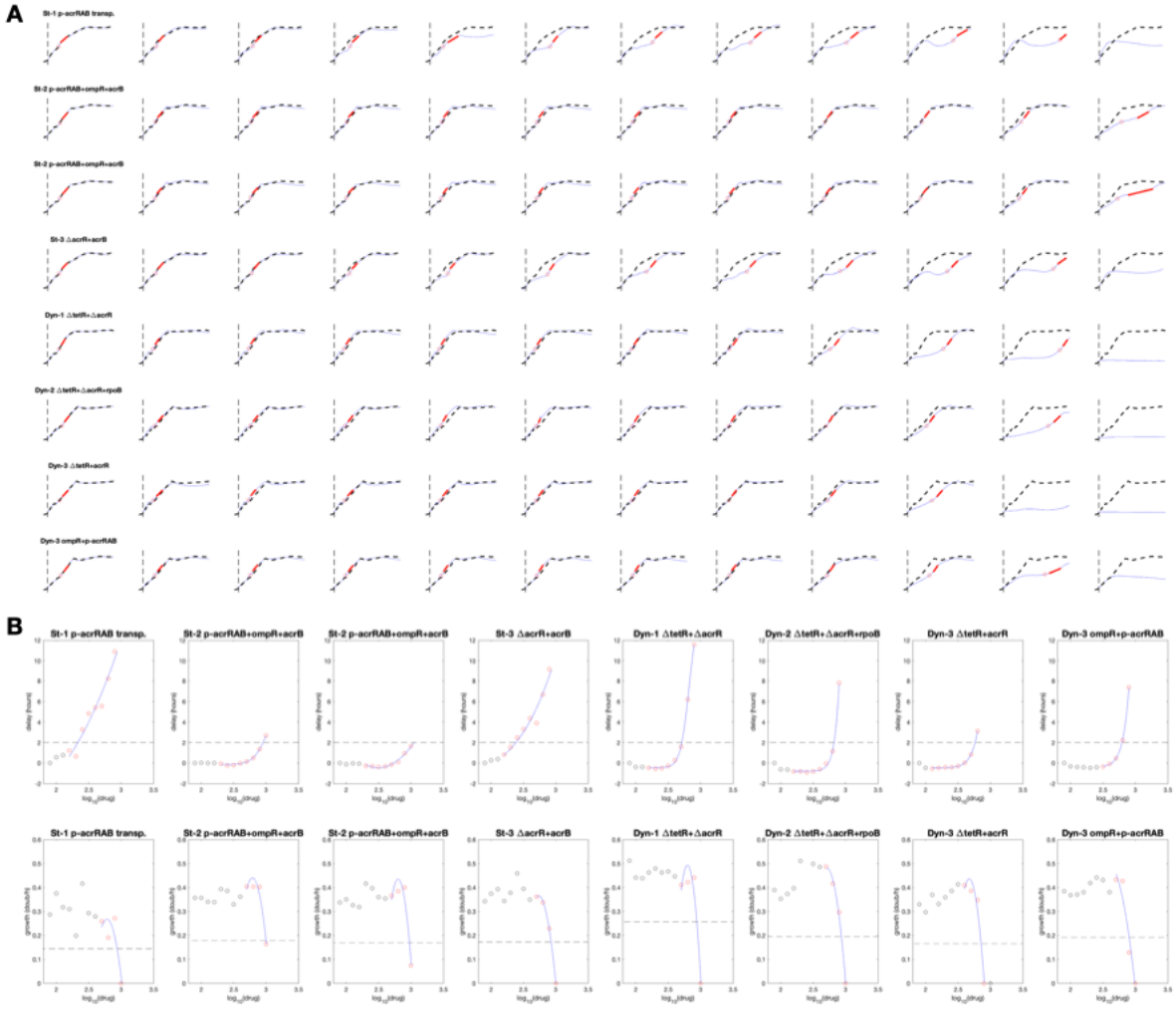

Figure S6. Calculation of steady-state and dynamical resistances for select mutants. A. Growth curves of select isolates picked from the final populations. Plots are $\log_2$(OD) over 20 hours. Vertical dashed line indicates addition of tetracycline picked from a gradient of zero in the first column then 100 to 1000 μg/ml in columns 2 to 12. The corresponding growth curve with zero drug is included in a dashed line for comparison. The point at which the culture reaches a doubling is indicated, as well as the linear fit during steady-state growth following recovery. **B.** Dynamic resistance is calculated as the drug concentration that causes a 2-hour delay in the time to reach one doubling following drug exposure. Steady-state resistance is calculated as the drug concentration that reduces steady-state growth to half of the growth rate under no drug. Curves were fit with second order polynomials.

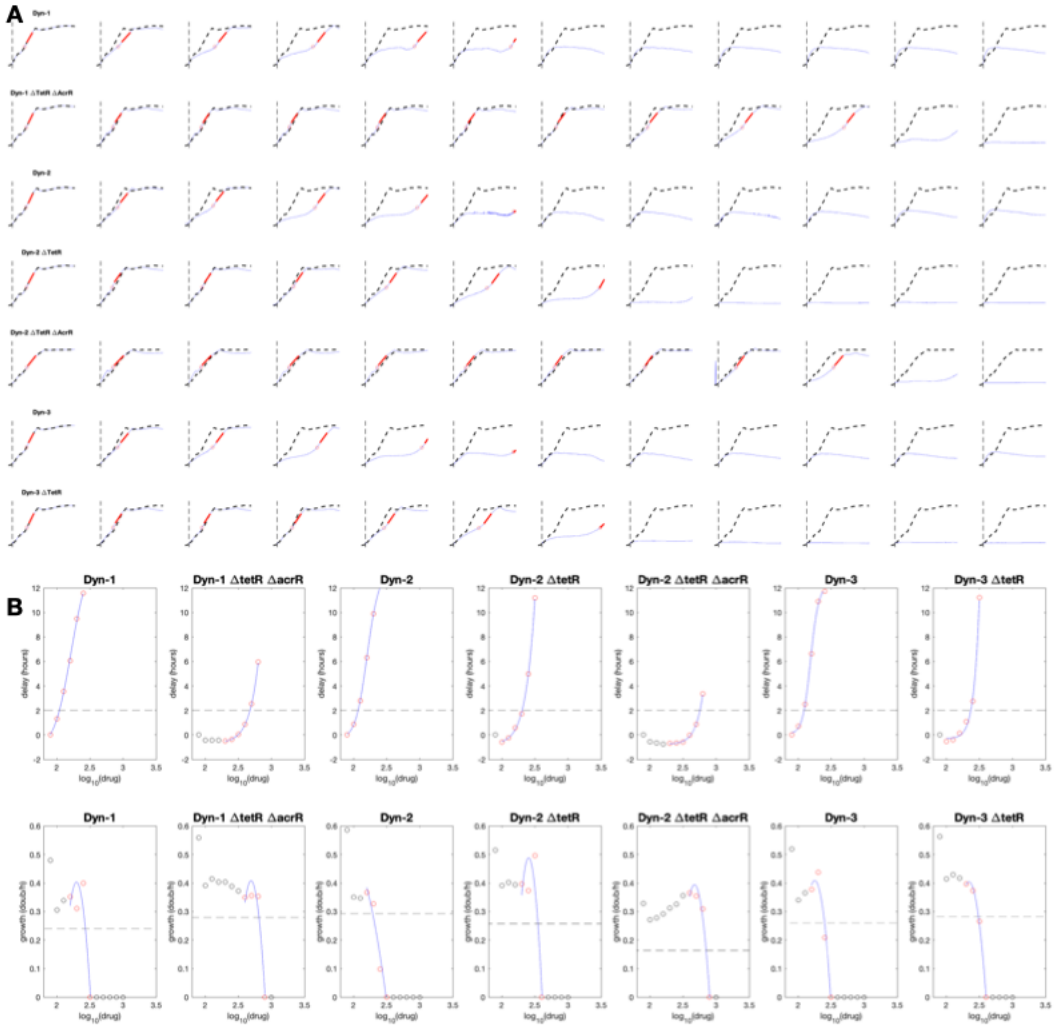

Figure S7. Calculation of gains in steady-state and dynamical resistances upon loss of TetR function. A. Growth curves of isolates picked in the same day, with and without transposon insertion in TetR, for each Dynamic population. Further acquisitions of AcrR mutations are also included. Plots are $\log_2$(OD) over 20 hours. Vertical dashed line indicates addition of tetracycline picked from a gradient of zero in the first column then 100 to 1000 µg/ml in columns 2 to 12. The corresponding growth curve with zero drug is included in a dashed line for comparison. The point at which the culture reaches a doubling is indicated, as well as the linear fit during steady-state growth following recovery. **B.** Dynamic resistance is calculated as the drug concentration that causes a 2-hour delay in the time to reach one doubling following drug exposure. Steady-state resistance is calculated as the drug concentration that reduces steady-state growth to half of the growth rate under no drug. Curves were fit with second order polynomials.